International Journal of Physical Sciences

October 2013 - Vol. 8 Num. 38

Submit manuscripts: www.ms.academicjournals.org

Editorial Office: ijps@academicjournals.org

URL: www.academicjournals.org

academicJournals

ABOUT IJPS

The **International Journal of Physical Sciences (IJPS)** is published weekly (one volume per year) by Academic Journals.

International Journal of Physical Sciences (IJPS) is an open access journal that publishes high-quality solicited and unsolicited articles, in English, in all Physics and chemistry including artificial intelligence, neural processing, nuclear and particle physics, geophysics, physics in medicine and biology, plasma physics, semiconductor science and technology, wireless and optical communications, materials science, energy and fuels, environmental science and technology, combinatorial chemistry, natural products, molecular therapeutics, geochemistry, cement and concrete research, metallurgy, crystallography and computer-aided materials design. All articles published in IJPS are peer-reviewed.

Submission of Manuscript

Submit manuscripts as e-mail attachment to the Editorial Office at: ijps@academicjournals.org. A manuscript number will be mailed to the corresponding author shortly after submission.

For all other correspondence that cannot be sent by e-mail, please contact the editorial office (at ijps@academicjournals.org).

The International Journal of Physical Sciences will only accept manuscripts submitted as e-mail attachments.

Please read the **Instructions for Authors** before submitting your manuscript. The manuscript files should be given the last name of the first author.

Editors

Editorial Board

Instructions for Author

Electronic submission of manuscripts is strongly encouraged, provided that the text, tables, and figures are included in a single Microsoft Word file (preferably in Arial font).

The **cover letter** should include the corresponding author's full address and telephone/fax numbers and should be in an e-mail message sent to the Editor, with the file, whose name should begin with the first author's surname, as an attachment.

Article Types

Three types of manuscripts may be submitted:

Regular articles: These should describe new and carefully confirmed findings, and experimental procedures should be given in sufficient detail for others to verify the work. The length of a full paper should be the minimum required to describe and interpret the work clearly.

Short Communications: A Short Communication is suitable for recording the results of complete small investigations or giving details of new models or hypotheses, innovative methods, techniques or apparatus. The style of main sections need not conform to that of full-length papers. Short communications are 2 to 4 printed pages (about 6 to 12 manuscript pages) in length.

Reviews: Submissions of reviews and perspectives covering topics of current interest are welcome and encouraged. Reviews should be concise and no longer than 4-6 printed pages (about 12 to 18 manuscript pages). Reviews are also peer-reviewed.

Review Process

All manuscripts are reviewed by an editor and members of the Editorial Board or qualified outside reviewers. Authors cannot nominate reviewers. Only reviewers randomly selected from our database with specialization in the subject area will be contacted to evaluate the manuscripts. The process will be blind review.

Decisions will be made as rapidly as possible, and the journal strives to return reviewers' comments to authors as fast as possible. The editorial board will re-review manuscripts that are accepted pending revision. It is the goal of the IJPS to publish manuscripts within weeks after submission.

Regular articles

All portions of the manuscript must be typed double-spaced and all pages numbered starting from the title page.

The Title should be a brief phrase describing the contents of the paper. The Title Page should include the authors' full names and affiliations, the name of the corresponding author along with phone, fax and E-mail information. Present addresses of authors should appear as a footnote.

The Abstract should be informative and completely self-explanatory, briefly present the topic, state the scope of the experiments, indicate significant data, and point out major findings and conclusions. The Abstract should be 100 to 200 words in length.. Complete sentences, active verbs, and the third person should be used, and the abstract should be written in the past tense. Standard nomenclature should be used and abbreviations should be avoided. No literature should be cited.

Following the abstract, about 3 to 10 key words that will provide indexing references should be listed.

A list of non-standard **Abbreviations** should be added. In general, non-standard abbreviations should be used only when the full term is very long and used often. Each abbreviation should be spelled out and introduced in parentheses the first time it is used in the text. Only recommended SI units should be used. Authors should use the solidus presentation (mg/ml). Standard abbreviations (such as ATP and DNA) need not be defined.

The Introduction should provide a clear statement of the problem, the relevant literature on the subject, and the proposed approach or solution. It should be understandable to colleagues from a broad range of scientific disciplines.

Materials and methods should be complete enough to allow experiments to be reproduced. However, only truly new procedures should be described in detail; previously published procedures should be cited, and important modifications of published procedures should be mentioned briefly. Capitalize trade names and include the manufacturer's name and address. Subheadings should be used. Methods in general use need not be described in detail.

Results should be presented with clarity and precision. The results should be written in the past tense when describing findings in the authors' experiments. Previously published findings should be written in the present tense. Results should be explained, but largely without referring to the literature. Discussion, speculation and detailed interpretation of data should not be included in the Results but should be put into the Discussion section.

The Discussion should interpret the findings in view of the results obtained in this and in past studies on this topic. State the conclusions in a few sentences at the end of the paper. The Results and Discussion sections can include subheadings, and when appropriate, both sections can be combined.

The Acknowledgments of people, grants, funds, etc should be brief.

Tables should be kept to a minimum and be designed to be as simple as possible. Tables are to be typed double-spaced throughout, including headings and footnotes. Each table should be on a separate page, numbered consecutively in Arabic numerals and supplied with a heading and a legend. Tables should be self-explanatory without reference to the text. The details of the methods used in the experiments should preferably be described in the legend instead of in the text. The same data should not be presented in both table and graph form or repeated in the text.

Figure legends should be typed in numerical order on a separate sheet. Graphics should be prepared using applications capable of generating high resolution GIF, TIFF, JPEG or Powerpoint before pasting in the Microsoft Word manuscript file. Tables should be prepared in Microsoft Word. Use Arabic numerals to designate figures and upper case letters for their parts (Figure 1). Begin each legend with a title and include sufficient description so that the figure is understandable without reading the text of the manuscript. Information given in legends should not be repeated in the text.

References: In the text, a reference identified by means of an author‘s name should be followed by the date of the reference in parentheses. When there are more than two authors, only the first author‘s name should be mentioned, followed by ’et al‘. In the event that an author cited has had two or more works published during the same year, the reference, both in the text and in the reference list, should be identified by a lower case letter like ’a‘ and ’b‘ after the date to distinguish the works.

Examples:

Abayomi (2000), Agindotan et al. (2003), (Kelebeni, 1983), (Usman and Smith, 1992), (Chege, 1998; 1987a,b; Tijani, 1993,1995), (Kumasi et al., 2001)
References should be listed at the end of the paper in alphabetical order. Articles in preparation or articles submitted for publication, unpublished observations, personal communications, etc. should not be included in the reference list but should only be mentioned in the article text (e.g., A. Kingori, University of Nairobi, Kenya, personal communication). Journal names are abbreviated according to Chemical Abstracts. Authors are fully responsible for the accuracy of the references.

Examples:

Ogunseitan OA (1998). Protein method for investigating mercuric reductase gene expression in aquatic environments. Appl. Environ. Microbiol. 64:695-702.
Gueye M, Ndoye I, Dianda M, Danso SKA, Dreyfus B (1997). Active N2 fixation in several Faidherbia albida provenances. Ar. Soil Res. Rehabil. 11:63-70.

Charnley AK (1992). Mechanisms of fungal pathogenesis in insects with particular reference to locusts. In: Lomer CJ, Prior C (eds) Biological Controls of Locusts and Grasshoppers: Proceedings of an international workshop held at Cotonou, Benin. Oxford: CAB International, pp 181-190.

Mundree SG, Farrant JM (2000). Some physiological and molecular insights into the mechanisms of desiccation tolerance in the resurrection plant Xerophyta viscasa Baker. In Cherry et al. (eds) Plant tolerance to abiotic stresses in Agriculture: Role of Genetic Engineering, Kluwer Academic Publishers, Netherlands, pp 201-222.

Short Communications

Short Communications are limited to a maximum of two figures and one table. They should present a complete study that is more limited in scope than is found in full-length papers. The items of manuscript preparation listed above apply to Short Communications with the following differences: (1) Abstracts are limited to 100 words; (2) instead of a separate Materials and Methods section, experimental procedures may be incorporated into Figure Legends and Table footnotes; (3) Results and Discussion should be combined into a single section.
Proofs and Reprints: Electronic proofs will be sent (e-mail attachment) to the corresponding author as a PDF file. Page proofs are considered to be the final version of the manuscript. With the exception of typographical or minor clerical errors, no changes will be made in the manuscript at the proof stage.

International Journal of Physical Sciences

Table of Contents: Volume 8 Number 38, 16 October, 2013

ARTICLES

academicJournals

Vol. 8(38), pp. 1873-1879, 16 October, 2013
DOI: 10.5897/IJPS2013.3898
ISSN 1992 - 1950 © 2013 Academic Journals
http://www.academicjournals.org/IJPS

International Journal of Physical Sciences

Full Length Research Paper

Convolutive cyclic voltammetry studies of PVA/CuI polymer composites at gold electrode

El-Hallag I. S.[1]*, El-Mossalamy E.H.[2], El-Mansy M. K.[3] and Al-Harbi L. M.[4]

[1]Department of Chemistry, Faculty of Science, Tanta University, Tanta 31527, Egypt.
[2]Department of Chemistry, Faculty of Science, Benha University, Benha, Egypt.
[3]Department of Physics, Faculty of Science, Benha University, Benha, Egypt.
[4]Department of Chemistry, Faculty of Science King Abdulaziz University, P. O. Box 42805, Jeddah 21551, Saudi Arabia.

Accepted 10 October, 2013

Cyclic voltammetry of PVA/CuI polymer composites was studied in acetonitrile as a solvent containing Tetrabutylammonium tetrafluoroborate (TBAFB). Cyclic voltammogram of PVA/CuI polymer composites exhibited unidirectional oxidative peak in the forward scan and irreversible reductive peak in the negative scan. The voltammetric behaviour explored that the electrode reaction of the investigated composite proceeds as EC mechanism. The highest occupied molecular orbital (HOMO) and the lowest unoccupied molecular orbital (LUMO) energy levels of the PVA/CuI nanocomposites were estimated from cyclic voltammetry. The chemical and electrochemical parameters of the investigated composite were determined and discussed using cyclic voltammetry, convolutive voltammetry and digital simulation methods.

Key words: Polymer composite, polyvinyl alcohol, cyclic voltammetry, convolutive voltammetry.

INTRODUCTION

Solid polymer electrolytes (SPEs) have been extensively studied for application in many electrochemical devices, such as cellular phones, smart credit cards, and laptop computers (Gray, 1991). The unique physical and chemical properties of nanoparticles, which are different from their bulk counterparts, offer excellent opportunities for chemical and biological sensing (Carusu, 2001; Storhoff and Mirkin, 1999). The facilitation of the electron transfer can significantly improve the sensitivity via introducing the nano-particles into the sensing interface (Kang et al., 2008; Park et al., 2005). The size controllability, chemical stability, high catalysis activity and surface tenability make them very advantageous for various electroanalytical and electrocatalytic applications (Park et al., 2005; Xiao et al., 2008).

Solar energy conversion devices based on organic semi-conductors has attracted great attention due to the advantages of light weight, flexibility and low cost of production with the possibility of fabricating large area devices based on solution processing. New materials and fabrication procedures leading to the substantial reduced cost of photovoltaic electricity could help drive a rapid expansion in the implementation of photovoltaic technology. The need to improve the light-to-electricity conversion efficiency requires the implementation of such materials and the exploration of new device architectures (Nielsen et al., 2010; Genes et al., 2007; Maggini et al., 2010; Krebs et al., 2010). It is well known that the electrical and optical properties of polymers can be improved to a desired limit through suitable doping (Blom et al., 1998). Further, polymers, on doping with metal nanoparticles, show novel and distinctive properties obtained from the unique combination of the inherent characteristics of polymers and properties of the metal nanoparticles (Gautam and Ram, 2010). Over the years, polyvinyl alcohol (PVA) polymers have attracted attention due to their variety of applications. PVA is a potential material having high dielectric strength, good charge

*Corresponding author. E-mail: ibrahimelhallag@yahoo.com

storage capacity and dopant-dependent electrical and optical properties. It has carbon chain backbone with hydroxyl groups attached to methane carbons; these OH groups can be a source of hydrogen bonding and hence assist the formation of polymer composite (Yang et al., 2006).

Cuprous iodide (CuI) is a versatile candidate in band gap materials (CuI, CuSCN, and $CuAlO_2$) that were identified in the preparation of optical properties of thin film. CuI belongs to the I–VII semiconductors with zinc blend structure. Conducting materials and optically transparent films aroused much interest in the capability of application in electronic devices such as liquid crystal displays, photovoltaic devices, photothermal collectors and so on. The most interesting nature of this compound is that an inorganic semiconductor and its coordination chemistry let it readily couple with many inorganic and organic ligands as well (Yang et al., 2006; Tennakone et al., 1998; Kumara et al., 2001, Tonooka et al., 2002; Dherea et al., 2010; Kamat, 1994).

The crucial factors for the use of a semiconducting material as an active layer in the solar cells are the band gap and optical absorption of the material. The relatively large band gap of polymer such as PVA limits the absorption of near-infrared light and thus lowers the light harvesting and therefore cannot be used as an active layer in organic solar cells. The control over the band gap is necessary while designing new materials for organic solar cells. The band gap engineering allows one to design and synthesize new materials with maximum overlap of absorption spectrum with the solar emission spectrum. It is often found that the synthesis of low band gap polymer is not only the solution to address this problem but also the position of highest occupied molecular orbital (HOMO) and lowest unoccupied molecular orbital (LUMO) limits the open-circuit voltage (Voc) of the photovoltaic cell. These two properties of organic materials can be controlled by introducing nanoinorganic salts or introducing alternative electron rich and electron-deficient units in the polymer backbone (Kanimozhi et al., 2010; Peiova and Grozdanov, 2005).

In the present work, the PVA polymer was prepared with and without the inorganic salt CuI nanoparticles to produce p-type PVA/CuI nanocomposite with suitable energy band gap which matches with the solar energy spectra. Cyclic voltammetry technique was used to characterize the PVA/CuI polymer composite. The chemical and electrochemical parameters were calculated and discussed as unprecedented calculation. Digital simulation and convolutive voltammetry were used to support, verify and confirm the calculated parameters and the nature of electrode reaction.

EXPERIMENTAL PROCEDURE

Chemicals

Tetrabutylammonium tetrafluoroborate (TBAFB) (Sigma) were used without further purification. A polyvinyl alcohol polymer (PVA 99.9%), acetonitrile (99.9%), dimethyl sulfoxide (DMSO 99.9%) and CuI (99.5%) used in the present study were purchased from Sigma–Aldrich. Solution of polyvinyl alcohol (PVA) was prepared by adding deionized distilled water to solid PVA $(C_2H_4O)_x$ (where x = 30,000–70,000, average molecular weight) and then stirred by a magnetic stirrer at room temperature for 2 h. The composite film was formed by drop casting of composite solution in dimethyl sulfoxide (DMSO) on the working electrode, Indium Tin Oxide, (ITO). In order to remove the residual Dimethyl sulfoxide (DMSO) from the composite film, we heated the composite film at 50°C over-night.

The structure of the polymer electrolyte layers was investigated and confirmed in previous work (Sheha et al., 2012) using X-ray diffraction via ShIMADZU diffractometer type XRD 6000, wave length 1.5418 ˚A. In addition, the surface morphology of these nanocomposites was also examined using scanning electron microscope, SEM (JOEL-JSM Model 5600) (Sheha et al., 2012).

Instrumentation

The electrochemical cyclic voltammetry was conducted on the electrochemical instrument linked to an EG & G model 283 Potentiostat at 20°C in a 0.1 mol. Acetonitrile solution of tetrabutylammonium tetrafluoroborate (TBAFB) as background electrolyte at potential scan rate of 100 mV/s using Ag/AgCl reference and platinum wire as counter electrodes, respectively. Indium tin oxide was used as working electrode.

Convolutive voltammetry and digital simulation of the data for cyclic voltammetric experiments was performed on PC computer using EG & G Condesim software package. The simulation procedure was carried out using finite differences techniques. Algorithms for the simulation program were coded and implemented into the condesim software package supplied by EG & G. A direct method of the determined electrochemical parameters was performed by generating the simulated cyclic voltammogram of PVA/CuI using the average values of electrochemical parameters extracted experimentally and comparing it with the voltammogram recorded experimentally.

RESULTS AND DISCUSSION

Cyclic voltammetry study

Cyclic voltammetry was performed on the PVA/CuI in order to assess its electroactivity. Cyclic voltammetry revealed the presence of one oxidation and one reduction waves as illustrated in the voltammogram shown in Figure 1. The range of the scan was between +2 V to -2 V with a scan rate of 0.1 $V.s^{-1}$. Cyclic voltammetry (CV) confirmed the presence of a charge capacity (area under CV curve) for the PVA/CuI. The curve also indicated the presence of an intrinsic redox reaction between the electrode and the PVA/CuI, at the potential applied between +2 V and -2 V, resulting in an ion exchange between the electrodes and the electrolytes in the solvents carrying the mobile charged carriers to and from the PVA/CuI.

Cyclic voltammogram of CuI/PVA polymer composite recorded in 0.1 mol L^{-1} TBAFB/ acetonitrile at indium tin oxide (ITO) electrode and scan rate of 0.1 V s^{-1} exhibited a single anodic peak (E_{pa} = 1.370 V) in the positive scan

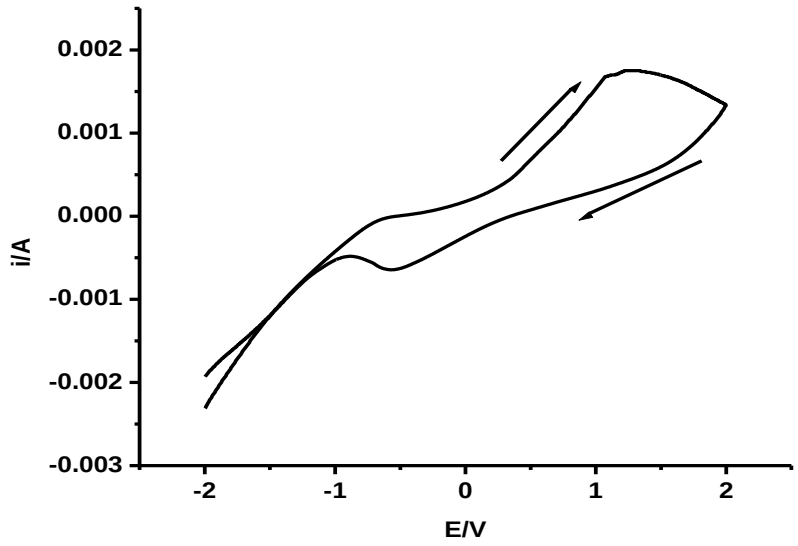

Figure 1. Cyclic voltammogram of PVA/CuI nanocomposite in CH3CN/0.1 M Tetrabutylammonium tetrafluoroborate **(**TBAFB**)** at sweep rate of 0.1 V.s^{-1}.

Table 1. Values of the electrochemical parameters of the investigated PVA/CuI polymer composite at ITO electrode.

Electrochemical parameter	Method							
	CV		Convolution		Deconvolution		Simulation	
	Ox	Red	Ox	Red	Ox	Red	Ox	Red
k_s x 10^6 ($cm.s^{-1}$)							3.53	2.65
D x10^6($cm^2.s^{-1}$)	2.32	3.23	2.75	3.26			2.13	3.45
E^0, V							0.71	-0.23
k_c , s^{-1}							0.05	0.04
Ep- Ep/2, V	0.550	0.252					0.554	0.257
$w^{1/2}$, V	0.397	0.320						
i_p,x10^3 A	1.70	1.21					1.73	1.25
E_p, V	1.35	0.50					1.36	0.52
I_{lim} x10^3, ($A.s^{-1/2}$)			4.1	2.5				

and a unidirectional cathodic peak (E_{pc} = - 0.510 V) in the negative scan at 20°C (Figure 1). Under normal circumstances, PVA exhibits one oxidation peak (Kanimozhi et al., 2010). The voltammogram depicted in Figure 1 exhibited two single redox waves. These redox waves may be due to more intricate reactions occurring between the PVA/CuI, the electrolytes and the electrode. The oxidative and reductive waves of the recorded cyclic voltammogram may be attributed to slow electron transfer followed by fast chemical reaction as indicated from the absence of counter peaks coupled with anodic and cathodic processes, that is, the electrode behaviour of the CuI/PVA polymer composites solution proceed as EC_{irr} mechanism for oxidation and reduction steps (El-Hallag and Hassanien, 1999).

The formal potential ($E^{0'}$), heterogeneous rate constant (k_s), the symmetry coefficient (α) and the homogeneous chemical rate constant (k_c) of oxidation and reduction steps were determined from simulated voltammograms and cited in Table 1. The generated theoretical cyclic voltammogram is indicated in Figure 2. In the selected scan rate (0.1 V.s^{-1}), the difference in the peak potential and half peak potential (E_p - $E_{p/2}$) of the anodic and the cathodic reactions were found to be 550 and 252 mV respectively. This behaviour may be due to the sluggish nature of the rate of electron transfer in addition to some uncompensated solution resistance of the CuI/PVA polymer composites solution (Oldham, 1983). Also the values of half peak width indicate that the oxidative process is slower than the reductive process.

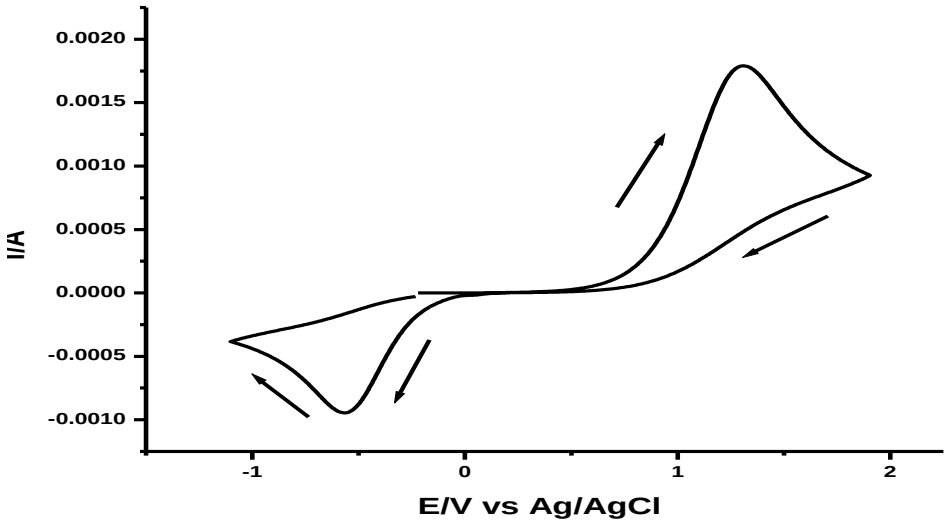

Figure 2. Simulated cyclic voltammogram of PVA/CuI polymer composite at sweep rate of 0.1 $V.s^{-1}$.

Effective charge transports from donor to acceptor component and charge collection at the electrodes are important parameters for designing and optimization of organic bulk heterojunction photovoltaic devices. In this regard, the electrochemical data gives valuable information and allow the estimation of relative position of HOMO/LUMO levels of the materials used for device fabrication. The knowledge of these levels is required for finding suitable donor-acceptor combination for the efficient bulk hetero-junction photo-voltaic device based on organic materials. The method of evaluation the HOMO and LUMO energy levels from the onset oxidation and reduction potentials have been proposed in literatures (Meng and Wudl, 2001). The position of HOMO and LUMO level has been determined from the analysis of redox potential behavior observed in cyclic voltammogram curve shown in Figure 1, using the expressions (1) and (2).

$$E_{HOMO} = -E_{OX}^{onset} - 4.75 \text{ eV} \quad (1)$$

$$E_{LUMO} = -E_{red}^{onset} - 4.75 \text{ eV} \quad (2)$$

Values of E_{OX}^{onset}, E_{red}^{onset}, E_{HOMO} and E_{LUMO} are 0.8, -0.23, -5.55 and -4.52 V respectively. Energy gap ($E_g = E_{LUMO} - E_{HOMO}$) in this material is found to be 1.05 eV. As indicated the cyclic voltammetry measurements have been performed to ascertain the position of both HOMO and LUMO levels which illustrated a movement of HOMO level towards vacuum level.

Convolution-deconvolution voltammetry

The convolution theorem finds use in the situation where it is required to perform the inverse transformation on a function which is the product of two functions of the Laplace variable each of which individually have known inverse transformations. In such a situation, the convolution theorem gives (Oldham, 1983; El-Hallag and Ghoneim, 1996)

$$L^{-1}[f_s(s).g_s(s)] = \int_0^t G(u)\,F(t-u)\,du \quad (3)$$

in which f_s, g_s are the Laplace transform of the functions F and G, the variable u is a dummy variable which is lost when the definite integral is evaluated. For the following reaction, in which a given species undergoing only electron transfer and no subsequent processes other than 'linear'

$$A + ne \longleftrightarrow B \quad (4)$$

diffusion out in the solution from a planar electrode, that is, the Fick's Second Law is expressed as (El-Hallag and Ghoneim, 1996)

$$[\partial C_A/\partial t]_x = D_A [\partial^2 C_A/\partial x^2]_x \quad (5)$$

then the solution of the above via Laplace methods yields

$$(C^{bulk} - C^s) = I_1 / n FSD^{1/2}_A \quad (6)$$

and

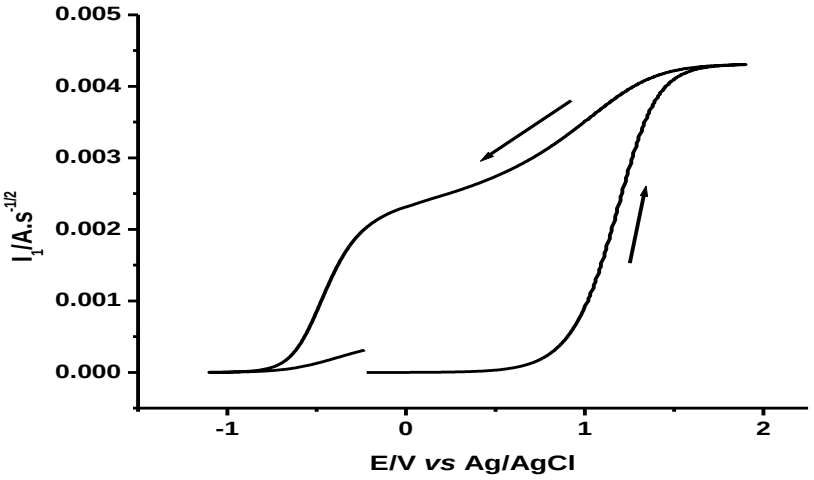

Figure 3. Convolution voltammetry (*I*1) of PVA/CuI polymer composite at sweep rate of 0.1 $V.s^{-1}$.

$$C^{bulk} = I_{lim} / n\,FSD^{1/2}{}_A \quad (7)$$

where C^{bulk} and C^s are the bulk and surface concentrations respectively and the convolution I_1 is given by $I_1 = i^*(\pi t)^{-1/2}$ or more 'fully' as:

$$I_1(t) = \pi^{-1/2} \int_0^t i(u) / (t-u)^{1/2} du \quad (8)$$

where I_1 (t) is the convoluted current at the total elapsed time (t), i (u) is the experimental current at time u and I_{lim} is the limiting value of I_1 at 'extreme' potentials; that is, when the concentration at the electrode C^s is effectively reduced to zero by rapid redox conversion and the current is thus controlled solely by the maximum rates of diffusion to and from the electrode. In the case of electron transfer followed by homogeneous reaction, the species here are produced by electron transfer at a planar electrode and convert into new product in the bulk via a chemical reaction with rate constant k_c. The Fick's Second Law expression is now (El-Hallag, 2009; Blagg et al., 1985):

$$[\partial C_B/\partial t]_x = D_B[\partial^2 C_B/\partial x^2]_x - k_c C_B \text{ (at x)} \quad (9)$$

and solution via Laplace methods gives here, necessarily starting at zero concentration in the bulk, the following electrode concentration in the bulk:

$$C^s{}_B = I_2 / nFAD^{1/2}{}_B \quad (10)$$

where the 'kinetic' convolution I_2 is given by Blagg et al., (1985).

$$I_2(t) = \pi^{-1/2} \int_0^t [i(u) \exp(-kc(t-u))]/(t-u)^{1/2} du \quad (11)$$

Thus in the I_2 convolution at time t, each segment of i(u) is scaled by dividing by the square root of the time which has elapsed from t to the time u to which the segment refers and likewise is scaled by the exponential factor $\exp(-k_c(t-u))$. Thus I_2 for example now goes to a plateau (at zero) on return of the sweep in cyclic voltammetry and this property allows determination of k_c in the case of the appearance of counter peaks coupled with anodic and/or cathodic peaks, otherwise the k_c is determined from digital simulation .

The diffusion coefficient of the investigated composite was determined, after applying background subtraction and correction for uncompensated resistance, from combination between cyclic voltammetry and convolution voltammetry via the following Equation 12 (Blagg et al., 1985; Doetsch, 1953; El-Hallag et al., 2000).

$$I_{lim} = i_p / 3.099(\alpha n_a v)^{1/2} \quad (12)$$

where I_{lim} is the limiting value achieved for I_1 when the potential is driven to a sufficiently extreme value past the peak, i_p is height of peak current of the cyclic voltammogram and the other terms has their usual meanings. The I_1 convolution of the investigated compound illustrated in Figure 3 shows a distinct separation between the forward and reverse sweep and clearly indicates the sluggishness of electron transfer of the electrode pathway. The reverse sweep of the I_1 convolution of both anodic and cathodic peaks does not return to zero due to the fast chemical reaction which

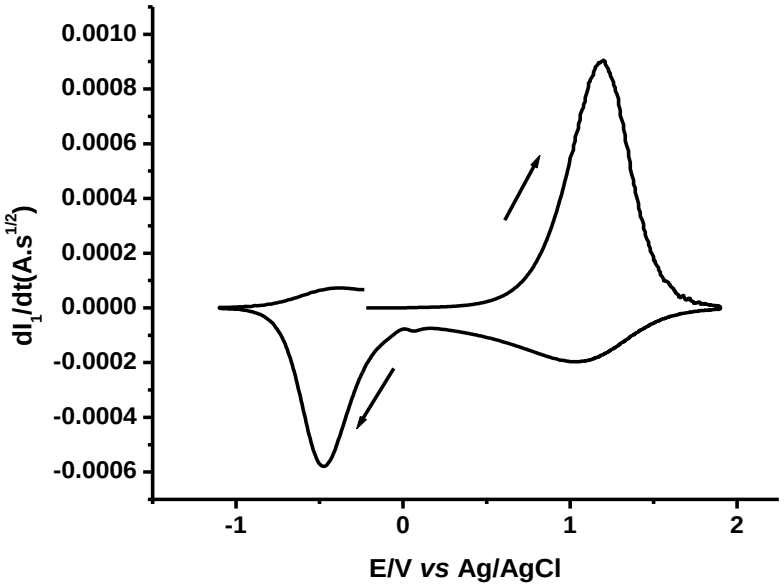

Figure 4. Deconvolution voltammetry (d/1/dt) of PVA/CuI polymer composite at sweep rate of 0.1 $V.s^{-1}$.

appears at time scales of the experiment. Value of the diffusion coefficient D evaluated via Equations 12 was found at 3.45 ± 0.5 $x10^{-6}$ cm^2s^{-1}. The homogeneous chemical rate constants (k^{ox}_c and k^{red}_c) of the chemical step that follows the charge transfer of both anodic and cathodic electrochemical reactions was calculated via digital simulation and listed in Table 1.

The deconvolution of current (dI_1/dt) can be expressed as the differential of the I_1 convolution. In more general terms, deconvolution is a kin to semi-differentiation in a similar manner to considering $t^{-1/2}$ convolution as semi-integration. The relationship between $t^{-1/2}$ convolutions and deconvolutions is indicated in the following scheme:

$$(dI_1/dt) \underset{\text{deconvolution}}{\overset{\text{convolution}}{\longleftrightarrow}} i \underset{\text{deconvolution}}{\overset{\text{convolution}}{\longleftrightarrow}} I_1\,(t)$$

Figure 4 indicates the deconvolution votammogram of the investigated polymer composite at 0.1 $V.s^{-1}$. It was found that the peak width ($w^{1/2}$) of andodic and cathodic process are equal 397 ± 4 mV and 320 ± 4 mV respectively. The measured values of $w^{1/2}$ are more than 90/n mV expected for one electron nernstain process confirming the slow nature of electron transfer (Saveant and Tessier, 1975).

Conclusion

In this article, CuI/PVA nanopolymer composites were prepared. The characterization of the composite using cyclic voltammetry and convolutive voltammetry was done as first time. The electrochemical band gap estimated from the cyclic voltammetry agrees well with the trend observed with the optical band gap established in literature. This can be easily understood in terms of the HOMO and LUMO energy levels of composites with respect to the work functions of both electrodes. From cyclic voltammetric measurements, it was concluded that the oxidation and reduction process proceeds as slow electron transfer followed by fast chemical process. The chemical and electrochemical parameters of polymer composite was determined and discussed.

REFERENCES

Blagg LA, Carr SW, Cooper GR, Dobson ID, Gill JB, Goodal DC, Shaw BL, Taylor N, Boddington T (1985). A mechanistic study on complexes of type mer-[Cr(CO)$_3$(η^2-L–L)(σ-L–L)] (where L–L = $Ph_2PCH_2PPh_2$, $Ph_2PNHPPh_2$, or $Ph_2PNMePPh_2$) using spectr-oscopic and convolutive electrochemical techniques. J. Chem. Soc. Dalton Trans. P. 1213.

Blom PWM, Schoo HFM, Matters M (1998). Electrical characterization of electroluminescent polymer/nanoparticle composite devices. Appl. Phys. Lett. 73:3914-3916.

Carusu F (2001). Nanoengineering of Particle Surfaces. Adv. Mater. 13:11- 22.

Dherea SL, Latthea SS, Kappenstein C, Mukherjee SK, Venkateswara Rao A (2010). Comparative studies on p-type CuI grown on glass and copper substrate by SILAR method. Appl. Surf. Sci. 256:3967–3971.

Doetsch G (1953). Laplace Transformation, Dover, New York.

El-Hallag IS (2009). Cyclic voltammetry, convolutive voltammetry, chronopotentiometry and digital simulation studies of [Pt(C≡C tol)$_2$ (dppm)$_2$ -Ir(CO)$_2$]$^+$$PF^{-6}$ complex. Chin. Sci. Bull. 541:3801-3807.

El-Hallag IS, Ghoneim MM (1996). Electrochemical investigation of N,N′-Propylene-*bis*-(salicylideneiminato) Mn(III) in phosphate buffer solutions. Monatsh fur Chemie. 127: 487 - 494.

El-Hallag IS, Ghoneim MM, Hammam E (2000). New method for the investigation of CE system via convolutive voltammetry combined with digital simulation. Anal. Chim. Acta. 414:173-180.
El-Hallag IS, Hassanien AM (1999). Electrochemical Studies of the Complex (OC-6-22)-W$(CO)_3$$(dppm)_2$ at a Glassy Carbon Electrode in CH_2Cl_2. Collect. Czech. Chem. Commun. 64:1953-1965.
Gautam A, Ram S (2010). Preparation and thermomechanical properties of Ag-PVA nanocomposite films. Mater. Chem. Phys. 119:266–271.
Genes S, Neugebauer H, Sariciftci NS (2007). Conjugated Polymer-Based Organic Solar Cells. Chem. Rev. 107:1324–1338.
Gray FM (1991). Solid Polymer Electrolytes - Fundamental and Technological Application, VCH, New York.
Kamat PV (1994). Interfacial charge transfer processes in colloidal semiconductor systems. Prog. React. Kinet. 19:277–316.
Kang Q, Yang L, Cai Q (2008). An electro-catalytic biosensor fabricated with Pt–Au Nanoparticle-decorated titania nanotube array. Bioelectrochem. 74:62-65.
Kanimozhi C, Balraju P, Sharma GD, Patil S (2010). Synthesis of Diketopyrrolopyrrole Containing Copolymers: A Study of Their Optical and Photovoltaic Properties. J. Phys. Chem. B. 114:3095–4003.
Krebs FC, Tromholt T, Jorgensen M (2010). Upscaling of polymer solar cell fabrication using full roll-to-roll processing. Nanoscale. 2:873–886.
Kumara GRRA, Konno A, Senadeera GKR, Jayaweere PVV, De Silva DBRA, Tennakone T (2001). Dye-sensitized solar cell with the hole collector p-CuSCN deposited from a solution in n-propyl sulphide. Sol. Energy Mater. Sol. Cells. 69:195–199.
Maggini R, Po M, Camaioni N (2010). Polymer Solar Cells: Recent Approaches and Achievements. J. Phys. Chem. C. 114:695–706.
Meng H, Wudl F (2001). A Robust Low Band Gap Processable n-Type Conducting Polymer Based on Poly (isothianaphthene). Macromolecules. 34:1810-1816.
Nielsen T.D, Fyenbo J, Wadstrøm M, Marie S, Pedersen M.S (2010). Manufacture, integration and demonstration of polymer solar cells in a lamp for the “Lighting Africa” initiative. Energy Environ. Sci. 3:512-525.
Oldham KB (1983). The extraction of kinetic parameters from chronoamperometric or chronocoulometric data. J. Electroanal. Chem. 145:9-20.
Park JE, Atobe M, Fuchigami T (2005). Sonochemical synthesis of conducting polymer–metal nanoparticles nanocomposite. Electrochim. Acta. 51:849-854.
Peiova B, Grozdanov I (2005). Three-dimensional confinement effects in semiconducting zinc selenide quantum dots deposited in thin-film form. Mater. Chem. Phys. 90:35–46.
Saveant JM, Tessier D (1975). Convolution potential sweep voltammetry V. Determination of charge transfer kinetics deviating from the Butler-Volmer behaviour. J. Electroanal. Chem. Interfacial Electrochem. 65:57-66.
Sheha E, Khoder H, Shanap TS, El- Shaarawy MG, El-Mansy M.K (2012). Structure, dielectric and optical properties of p-type (PVA/CuI) nanocomposite polymer electrolyte for photovoltaic cells. Optik – Int. J Light and Electron Optics123:1161-1166.
Storhoff J, Mirkin CA (1999). Programmed Materials Synthesis with DNA. Chem. Rev. 99:1849-1862.
Tennakone K, Kumara GRRA, Kottegoda IRM, Perera VPS, Aponsu GMLP, Wijayantha KGU (1998). Deposition of thin conducting films of CuI on glass. Energy Mater. Sol. Cells. 55:283-289.
Tonooka K, Shimokawa K, Nishimura O (2002). Properties of copper–aluminum oxide films prepared by solution methods. Thin Solid Films, 411:129–133.
Xiao F, Zhao F, Li J, Liu L, Zeng B (2008). Characterization of hydrophobic ionic liquid-carbon nanotubes–gold nanoparticles composite film coated electrode and the simultaneous voltammetric determination of guanine and adenine. Electrochim. Acta. 53:7781–7788.
Yang Y, Zi Wang Z, Yan Gao Y, Liu T, Hu C, Dong Q (2006). Synthesis of fluorinated diblock copolymer by ATRP and its application of PAVAc polymerization in ScCO2. J. Appl. Polym. Sci. 2:1146–1151.

academicJournals

Vol. 8(38), pp. 1880-1884, 16 October, 2013
DOI: 10.5897/IJPS2013.4042
ISSN 1992 - 1950 © 2013 Academic Journals
http://www.academicjournals.org/IJPS

International Journal of Physical Sciences

Full Length Research Paper

Differential transform method for solving non-linear systems of partial differential equations

Raslan K. R.[1] and Zain F. Abu Sheer[2]

[1]Department of Mathematics, Faculty of Science, Al-Azhar University, Egypt.
[2]Department of Mathematics, preparatory year, Riyadh, King Saud University, Saudi Arabia.

Accepted 10 October, 2013

The differential transform method (DTM) has been applied to solve many functional equations so far. In this paper, we propose this method (DTM), for solving nonlinear Jaulent-Miodek and the Hirota-Satsuma equation. Numerical solutions obtained by differential transform method are compared with the exact solutions and that obtained by Adomian decomposition methods. The results for some values of the variables are shown in tables and the solutions are presented as plots as well, showing the ability of the method.

Key words: Differential transform method, Jaulent-Miodek (JM) equation, the Hirota-Satsuma equation, numerical.

INTRODUCTION

The differential transform method has been successfully used by Zhou (1986) to solve linear and nonlinear initial value problems in electric circuit analysis. In recent years, differential transform method (DTM) has been used to solve one-dimensional planar Bratu problem, differential-difference equation, delay differential equations, differential algebraic equation, integro-differential systems (Rostam et al., 2011; Kanth and Aruna, 2008; Zhou, 1986; Raslan and Zain, 2013; Raslan et al., 2012; Arikoglu and Ozko, 2008; Adbel-Halim, 2008; Wazwaz, 2000). We reformulate DTM to solve nonlinear Jaulent-Miodek and the Hirota-Satsuma equation and compare our results with the exact solutions.

The structure of this paper is organized as follows: firstly, we begin with some basic definitions and the use of the proposed method. Later, we apply the differential transformation method to solve Jaulent -Miodek(JM) equation and the Hirota-Satsuma equation in order to show its ability and efficiency.

DESCRIPTION OF THE METHODS

The differential transform method (DTM)

The differential transformation of the kth-order derivative of function $u(x)$ is defined as follows:

$$U(k) = \frac{1}{k!}\left[\frac{d^k u(x)}{dx^k}\right]_{x=x_0} \quad (1)$$

Where $u(x)$ is the original function, $U(k)$ is the transformed function and $\frac{d^k}{dx^k}$ is the kth derivative with respect to x .The differential inverse transform of $U(k)$ is defined as:

$$u(x) = \sum_{k=0}^{\infty} U(k)\,(x - x_0)^k, \quad (2)$$

*Corresponding author. Email: zainfathi@hotmail.com, zabusheer.c@ksu.edu.sa

Combining Equations 1 and 2 we obtain

$$u(x) = \sum_{k=0}^{\infty} \frac{1}{k!}\left[\frac{d^k u(x)}{dx^k}\right](x - x_0)^k \quad \text{at } x = x_0 \qquad (3)$$

The following theorems that can be deduced from Equations 1 and 2 are given (Rostam et al., 2011; Kanth and Aruna, 2008; Raslan and Zain, 2013; Raslan et al., 2012).

Theorem 1: If the original function is $u(x) = w(x) \pm v(x)$, then the transformed function is $U_k(x) = W_k(x) \pm V_k(x)$.

Theorem 2: If the original function is $u(x) = a\, v(x)$. then the transformed function is $U_k(x) = aV_k(x)$.

Theorem 3: If the original function is $u(x) = \frac{\partial^m w(x)}{\partial x^m}$. then the transformed function is $U_k(x) = \frac{(k+m)!}{k!} W_k(x)$.

Theorem 4: If the original function is $u(x) = \frac{\partial}{\partial x} w(x)$, then the transformed function is. $U_k(x) = \frac{\partial}{\partial x} W_k(x)$

Theorem 5: If the original function is $u(x) = x^n$, then the transformed function is

$$U(k) = \delta(k - n) = \begin{cases} 1 & k = n \\ 0 & k \neq n \end{cases}.$$

Theorem 6: If the original function is $u(k) = w(x,t)v(x,t)$, then the transformed function is

$$U_k(x) = \sum_{r=0}^{k} W_r(x) V_{k-r}(x)$$

APPLICATIONS

In this section, we propose the extended DTM, for solving Jaulent-Miodek(JM) equation and the Hirota-Satsuma equation. Numerical solutions obtained by the DTM are compared with the exact solutions, and compared with that obtained by Adomian decomposition methods (ADM) methods (Jafar and Mostfa, 2011; Raslan, 2004). The results for some values of the variables are shown in tables and the solutions are presented as plots as well, showing the ability of the method.

Consider the following Jaulent-Miodek equation (Jafar and Mostfa, 2011)

$$\frac{\partial u}{\partial t} + \frac{\partial^3 u}{\partial x^3} + \frac{3}{2} v \frac{\partial^3 u}{\partial x^3} + \frac{9}{2} \frac{\partial v}{\partial x} \frac{\partial^2 v}{\partial x^2} - 6u \frac{\partial u}{\partial x} - 6u v \frac{\partial v}{\partial x} - \frac{3}{2} \frac{\partial u}{\partial x} v^2 = 0,$$

$$\frac{\partial v}{\partial t} + \frac{\partial^3 v}{\partial x^3} - 6v \frac{\partial u}{\partial x} - 6u \frac{\partial v}{\partial x} - \frac{15}{2} \frac{\partial v}{\partial x} v^2 = 0 \qquad (4)$$

with an initial condition

$$u(x,0) = \frac{1}{4}\alpha - \frac{1}{4}\beta^2 - \frac{1}{2}\beta\sqrt{\alpha}\sec h(\sqrt{\alpha}x) - \frac{3}{4}\alpha \sec h^2(\sqrt{\alpha}x), \qquad (5)$$
$$v(x,0) = \beta + \sqrt{\alpha}\sec h(\sqrt{\alpha}x).$$

with the exact solution

$$u(x,t) = \frac{1}{4}(\alpha - \beta^2) - \frac{1}{2}\beta\sqrt{\alpha}\sec h(\sqrt{\alpha}(x + \gamma t)) - \frac{3}{4}\alpha \sec h^2(\sqrt{\alpha}(x + \gamma t)),$$
$$v(x,t) = \beta + \sqrt{\alpha}\sec h(\sqrt{\alpha}(x + \gamma t)).$$

Then, by using the basic properties of the reduced differential transformation, we can find the transformed form of Equation 4 as

$$(k+1)U_k = -\frac{\partial^3}{\partial x^3} U_k(x) - \frac{3}{2}\sum_{r=0}^{k}(V_{k-r}\frac{\partial^3 V_k}{\partial x^3}) - \frac{9}{2}\sum_{r=0}^{k}(\frac{\partial V_{k-r}}{\partial x}\frac{\partial^2 V_r}{\partial x^2})$$
$$+ 6\sum_{r=0}^{k}(U_{k-r}\frac{\partial U_k}{\partial x}) + 6\sum_{s=0}^{k}\sum_{r=0}^{s}(U_{k-r}V_{k-s}\frac{\partial V_k}{\partial x}) + \frac{3}{2}\sum_{s=0}^{k}\sum_{r=0}^{s}(V_{k-r}V_{k-s}\frac{\partial U_k}{\partial x})$$

$$(k+1)V_k = -\frac{\partial^3 V_k}{\partial x^3} + \sum_{r=0}^{k}(V_{k-r}\frac{\partial U_k}{\partial x}) + \sum_{r=0}^{k}(U_{k-r}\frac{\partial V_k}{\partial x})$$
$$+ \frac{15}{2}\sum_{s=0}^{k}\sum_{r=0}^{s}(V_{k-r}V_{k-s}\frac{\partial V_k}{\partial x}) \qquad (6)$$

Using the initial condition (5), we have

$$U_0 = \frac{1}{4}\alpha - \frac{1}{4}\beta^2 - \frac{1}{2}\beta\sqrt{\alpha}\sec h(\sqrt{\alpha}\,x) - \frac{3}{4}\alpha \sec h^2(\sqrt{\alpha}\,x), \qquad (7)$$
$$V_0 = \beta + \sqrt{\alpha}\sec h(\sqrt{\alpha}\,x).$$

Now, substituting Equation 7 into Equation 6, we obtain the following $U_k(x)$ values successively

$$U_1 = \frac{1}{4}\big(-3\alpha^2\beta\,\mathrm{sech}[x\sqrt{\alpha}]\tanh[x\sqrt{\alpha}] + 6\alpha\beta^3\,\mathrm{sech}[x\sqrt{\alpha}]\tanh[x\sqrt{\alpha}] + 3\alpha^{5/2}\mathrm{sech}[x\sqrt{\alpha}]^2\tanh[x\sqrt{\alpha}]$$
$$+ 18\alpha^{3/2}\beta^2\mathrm{sech}[x\sqrt{\alpha}]^2\tanh[x\sqrt{\alpha}] + 4\alpha^2\beta\,\mathrm{sech}[x\sqrt{\alpha}]^3\tanh[x\sqrt{\alpha}]$$
$$+ 4\alpha^2\beta\,\mathrm{sech}[x\sqrt{\alpha}]\tanh[x\sqrt{\alpha}]^3\big)$$

$$V_1 = \frac{1}{2}(-3\alpha^2\mathrm{Sech}[x\sqrt{\alpha}]\mathrm{Tanh}[x\sqrt{\alpha}] - 6\alpha\beta^2\mathrm{Sech}[x\sqrt{\alpha}]\mathrm{Tanh}[x\sqrt{\alpha}] + 2\alpha^2\mathrm{Sech}[x\sqrt{\alpha}]^3\mathrm{Tanh}[x\sqrt{\alpha}]$$
$$+ 2\alpha^2\mathrm{Sech}[x\sqrt{\alpha}]\mathrm{Tanh}[x\sqrt{\alpha}]^3) \qquad (8)$$

Substituting Equation 6 into Equation 3, we obtain the following $U_2(x)$ and $V_2(x)$ values successively. Finally the differential inverse transform of $U_k(x)$ and $V_k(x)$ gives:

$$u_n(x,t) = \sum_{k=0}^{\infty} U_k\ t^k \quad , \ v_n(x,t) = \sum_{k=0}^{\infty} V_k\ t^k \qquad (9)$$

For numerical study, terms approximations have been considered, and the results are presented in Tables 1 to 2 and Figures 1 to 2.

Table 1. The numerical results un(x,t) and vn(x,t) in comparison with the analytical solution u(x,t)and v(x,t), when $\alpha = \beta = 0.01$ [6]for solution of Equation 1.

x	T	Uexact.	Uapprox.	Abs. error	Vexact.	Vapprox.	Abs. error.
0.1	0.1	-0.00552422	-0.00552422	-7.31186×10^{-15}	0.109995	0.109995	4.09811×10^{-14}
0.1	0.15	-0.00552421	-0.00552421	-1.64166×10^{-14}	0.109995	0.109995	9.20652×10^{-14}
0.15	0.1	-0.00552324	-0.00552324	-1.74314×10^{-14}	0.109989	0.109989	1.03195×10^{-13}
0.2	0.3	-0.00552185	-0.00552185	-2.85525×10^{-13}	0.10998	0.10998	1.73363×10^{-12}
0.35	0.25	-0.00551544	-0.00551544	-6.2866×10^{-13}	0.109938	0.109938	3.92535×10^{-12}
0.45	0.45	-0.00550916	-0.00550916	-3.38924×10^{-12}	0.109898	0.109898	2.13474×10^{-11}
0.45	0.7	-0.00550907	-0.00550907	-8.18441×10^{-12}	0.109897	0.109897	5.15872×10^{-11}
0.8	0.8	-0.00547509	-0.00547509	-3.39431×10-11	0.109677	0.109677	2.16775×10^{-10}
0.85	0.95	-0.00546861	-0.00546861	-5.39471×10^{-11}	0.109636	0.109636	3.45017×10^{-10}
0.9	0.9	-0.0054619	-0.0054619	-5.42248×10^{-11}	0.109592	0.109592	3.47153×10^{-10}
1	1	-0.00544719	-0.00544719	-8.23443×10^{-11}	0.109497	0.109497	5.28343×10^{-10}

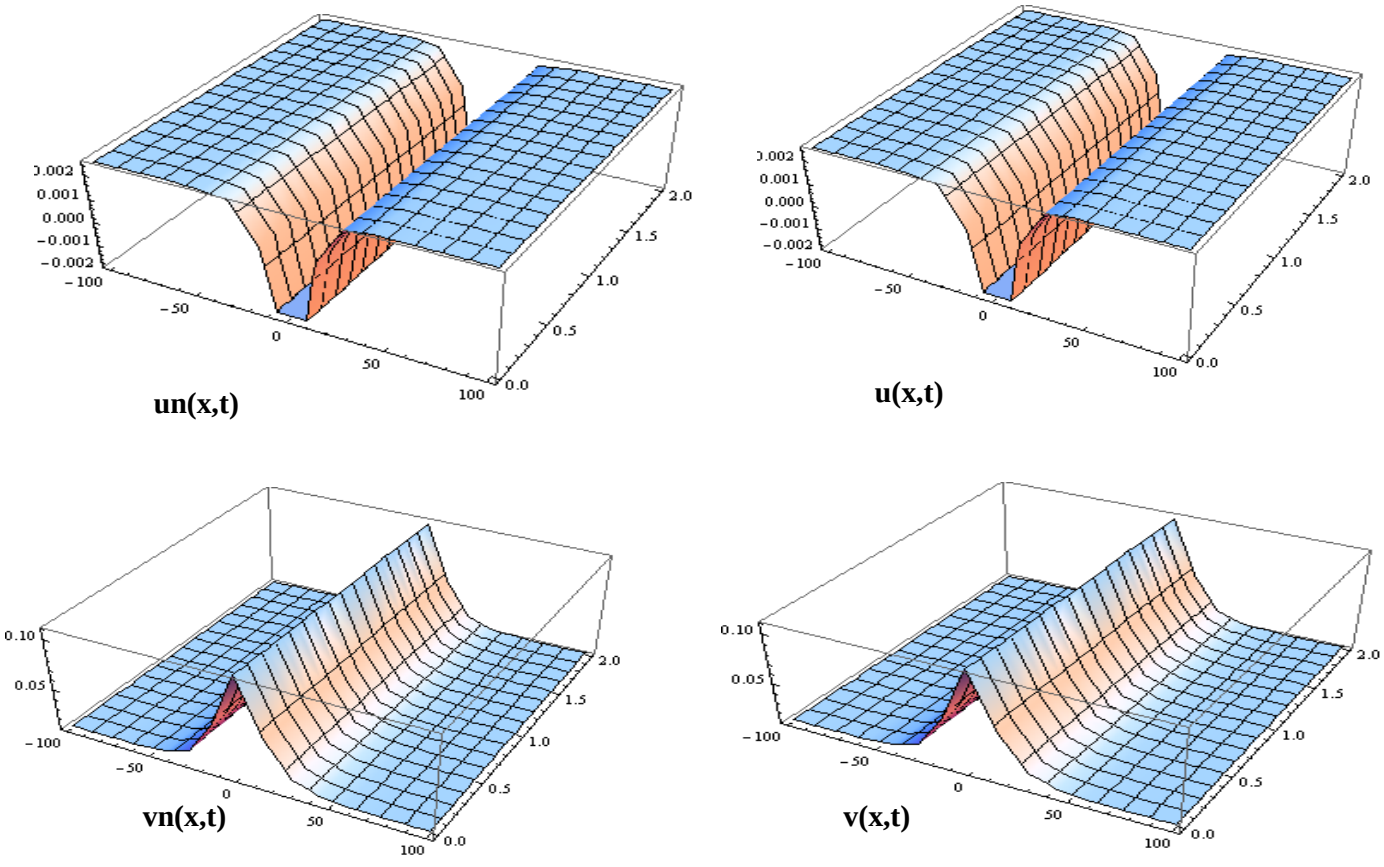

Figure 1. The numerical results for un(x,t) and vn(x,t) in comparison with the analytical solution u(x,t) and v(x,t).

Consider the Hirota-Satsuma equation (Raslan, 2004)

$$\frac{\partial u}{\partial t} = \frac{1}{2}\cdot\frac{\partial^3 u}{\partial x^3} - 3u\frac{\partial\ u}{\partial x} + 3v\frac{\partial w}{\partial x} + 3w\frac{\partial v}{\partial x},$$

$$\frac{\partial v}{\partial t} = -\frac{\partial^3 v}{\partial x^3} + 3u\frac{\partial v}{\partial x} \qquad (10)$$

$$\frac{\partial w}{\partial t} = -\frac{\partial^3 w}{\partial x^3} + 3u\frac{\partial w}{\partial x}$$

Table 2. Comparison between the approximation solutions (DTM) and approximation solutions (ADM) when $\alpha = \beta = \eta = 1, \xi$=0.1 and t =1 (Raslan, 2004).

X	Approximation solutions (DTM),N=4			Approximation solutions (ADM),N=4		
	Uapprox.	Vapprox.	Wapprox.	Uapprox.	Vapprox.	Wapprox.
-50	0.346645	0.0657245	1.99978	0.346645	0.0657245	1.99978
-40	0.346506	0.0656679	1.99836	0.346505	0.0656678	1.99836
-30	0.345492	0.0652524	1.98798	0.345487	0.0652518	1.98796
-20	0.338608	0.0623122	1.91447	0.338603	0.0623089	1.91437
-10	0.310292	0.0462485	1.51288	0.310816	0.0462566	1.51308
0	0.307185	0.0261333	1.01000	0.307183	0.0261307	1.00993
10	0.348145	0.0513519	1.64047	0.348596	0.0513653	1.64080
20	0.348941	0.0634004	1.94168	0.348992	0.0634044	1.94178
30	0.347039	0.0654094	1.9919	0.347044	0.0654099	1.9919 2
40	0.346718	0.0656893	1.9989	0.346719	0.0656894	1.99890
50	0.346674	0.0657274	1.99978	0.346674	0.0657274	1.99985

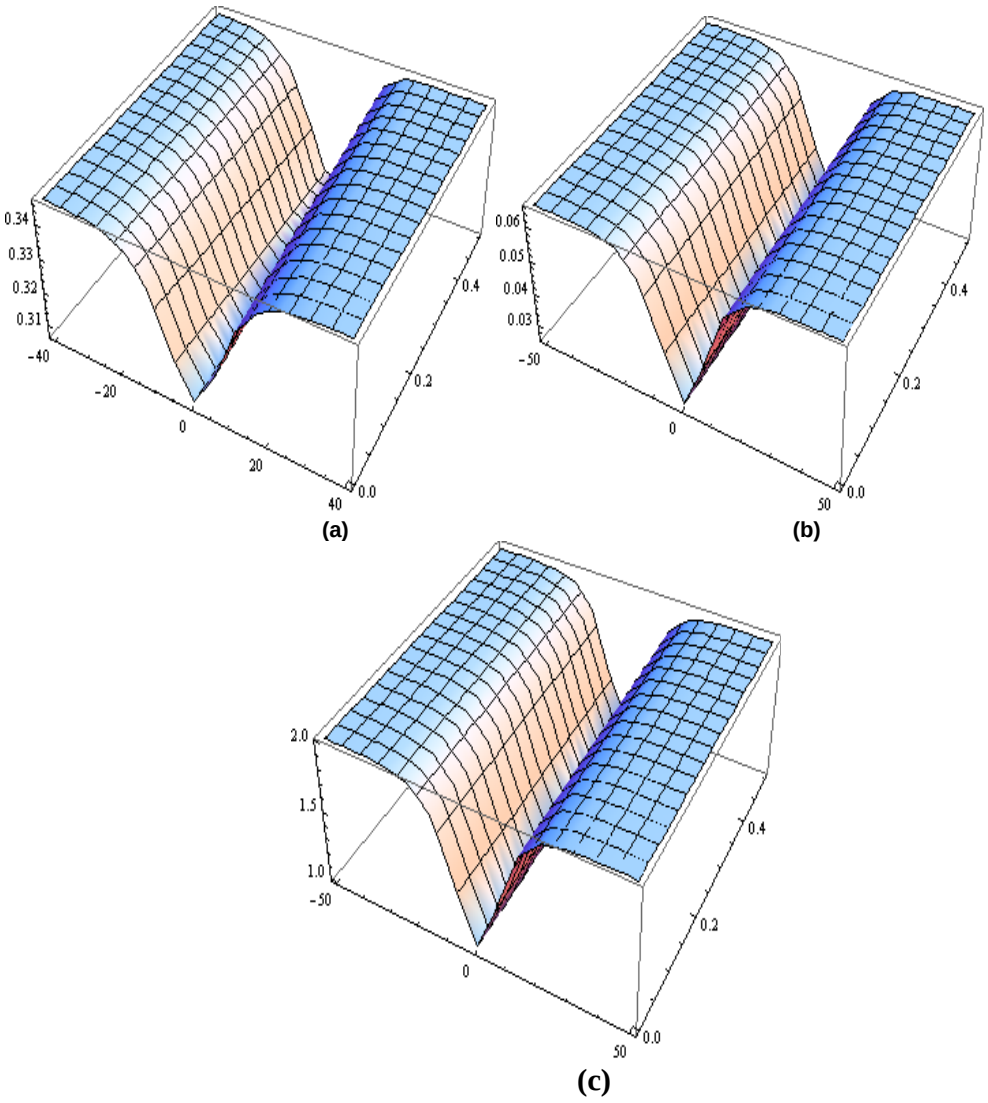

Figure 2. The approximation solutions of un(x,t), vn(x,t) and wn(x

with an initial condition

$$u(x,0) = \frac{1}{3}(\beta - 8\xi^2) + 4\xi^2 \tanh^2(\xi x),$$
$$v(x,0) = \frac{-4(3\alpha\xi^4 - 2\beta\eta\xi^2 + 4\eta\xi^4)}{3\eta^2} + \frac{4\xi^2}{\eta}\tanh^2(\xi x), \quad (11)$$
$$w(x,0) = \alpha + \eta\tanh^2(\xi x),$$

Then, by using the basic properties of the reduced differential transformation, we can find the transformed form of Equation 10 as

$$(k+1)U_k = \frac{1}{2}\frac{\partial^3}{\partial x^3}U_k(x) - 3\sum_{r=0}^{k}(U_{k-r}\frac{\partial U_r}{\partial x})) + 3\sum_{r=0}^{k}(V_{k-r}\frac{\partial W_k}{\partial x}) + 3\sum_{r=0}^{k}(W_{k-r}\frac{\partial V_k}{\partial x}), \quad (12)$$

$$(k+1)V_k = -\frac{\partial^3 V_k}{\partial x^3} + 3\sum_{r=0}^{k}(U_{k-r}\frac{\partial V_k}{\partial x}),$$

$$(k+1)W_k = -\frac{\partial^3 W_k}{\partial x^3} + 3\sum_{r=0}^{k}(U_{k-r}\frac{\partial W_k}{\partial x})$$

Using the initial condition (11), we have

$$U_0 = \frac{1}{3}(\beta - 8\xi^2) + 4\xi^2\tanh^2(\xi x),$$
$$V_0 = \frac{-4(3\alpha\xi^4 - 2\beta\eta\xi^2 + 4\eta\xi^4)}{3\eta^2} + \frac{4\xi^2}{\eta}\tanh^2(\xi x) \quad (13)$$
$$W_0 = \alpha + \eta\tanh^2(\xi x),$$

Now, substituting Equation 13 into Equation 12, we obtain the following $U_k(x)$ values successively

$$U_1 = -\frac{1}{\eta}8(-3\alpha\xi^3\text{Sech}[x\xi]^2\text{Tanh}[x\xi] - \beta\eta\xi^3\text{Sech}[x\xi]^2\text{Tanh}[x\xi] + 3\alpha\xi^5\text{Sech}[x\xi]^2 \\ 4\eta\xi^5\text{Sech}[x\xi]^2\text{Tanh}[x\xi] + 4\eta\xi^5\text{Sech}[x\xi]^4\text{Tanh}[x\xi] - 6\eta\xi^3\text{Sech}[x\xi]^2\text{Tanh}[x\xi]^3 + \\ 10\eta\xi^5\text{Sech}[x\xi]^2\text{Tanh}[x\xi]^3)$$

$$V_1 = \frac{8(\beta\xi^3\text{Sech}[x\xi]^2\text{Tanh}[x\xi] - 8\xi^5\text{Sech}[x\xi]^2\text{Tanh}[x\xi] + 8\xi^5\text{Sech}[x\xi]^4\text{Tanh}[x\xi] \\ +8\xi^5\text{Sech}[x\xi]^2\text{Tanh}[x\xi]^3)}{\eta} \quad (14)$$

$$W_1 = 2(\beta\eta\xi\text{Sech}[x\xi]^2\text{Tanh}[x\xi] - 8\eta\xi^3\text{Sech}[x\xi]^2\text{Tanh}[x\xi] + 8\eta\xi^3\text{Sech}[x\xi]^4\text{Tanh}[x\xi] \\ + 8\eta\xi^3\text{Sech}[x\xi]^2\text{Tanh}[x\xi]^3)$$

Substituting Equation 14 into Equation 12, we obtain $U_2(x)$ and $V_2(x)$ values. Finally the differential inverse transform of $U_k(x)$ and $V_k(x)$ gives:

$$un(x,t) = \sum_{k=0}^{\infty}U_k\ t^k\ ,\ vn(x,t) = \sum_{k=0}^{\infty}V_k\ t^k\ ,\ wn(x,t) = \sum_{k=0}^{\infty}W_k\ t^k \quad (15)$$

Conclusion

The DTM has been successfully applied for solving the nonlinear Jaulent-Miodek and the Hirota-Satsuma equation. The solutions obtained by DTM are compared with the exact solution. The results show that DTM method is a powerful mathematical tool for solving systems of nonlinear partial differential equations, which appears in mathematical modeling of different phenomena. These models have been solved by homotopy perturbation method and by Adomian's method. DTM method in comparison with ADM and HPM has the advantage of overcoming the difficulty arising in calculating ADM and HPM.

REFERENCES

Adbel-Halim IHH (2008). Comparison differential transform technique with Adomian decomposition method for linear and nonlinear intial value problem. Chaos Solitons Fractals, 36:53.

Arikoglu A, Ozko I (2008). Solution of integral and integro- differential systems by using differential transform method. Int. J. Comput. 56:2411.

Jafar B, Mostfa E (2011). A reliable algorithm for solving nonlinear Jaulent-Miodek equation. J.k.s.u-Science, 23:133.

Kanth ASVR, Aruna K (2008). Differential transform method for solving linear and non-linear systems of partial differential equations. Int. J. Phys. Sci. A (372):6896.

Raslan K, Biswas A, Zain FAS (2012). Differential transform method for solving partial differential equations with variable coefficients. Int. J. Phys. Sci. 9:1412.

Raslan KR (2004). The decomposttion method for a Hirota-satsuma coupled KdV equation and a coupled MKdV equation. Int. J. Comput. Math. 81:1497.

Raslan KR, Zain FAS (2013). Comparison study between differential transform method and Adomian decomposition method for some delay differential equations. Int. J. Phys. Sci. 17:744.

Rostam K, Saeed B, Rahman M (2011). Differential transform method for solving system of delay differential equation. Aust. J. Basic Appl. Sci. 4:201.

Wazwaz AM (2000). The decomposition method applied to systems of partial differential equations and to the reaction- diffusion Brusselator model. Appl. Math. Comput. 110:251.

Zhou JK (1986). Differential Transform and its Applications for Electrical Circuits Huazhong Univ. Press, Wuhan.

academicJournals

Vol. 8(38), pp. 1885-1891, 16 October, 2013
DOI: 10.5897/IJPS2013.3997
ISSN 1992 - 1950 © 2013 Academic Journals
http://www.academicjournals.org/IJPS

International Journal of Physical Sciences

Full Length Research Paper

Equivalence principle of light's momentum harmonizing observation from quantum theory to cosmology

Shinsuke Hamaji

Hyama Natural Science Research Institute, 403, Daiichi-Kiriya Building, 5-2, Chuo 2-chome, Nakano-ku, Tokyo 164-0011, Japan.

Accepted 10 October, 2013

Unlike in Newtonian mechanics, in the theory of relativity, the coordinate axis is not fixed, and the time axis serves as the background for the observation. In other words, the theory of relativity is background independent (BI). The quantum theory created in the micro-world, in contrast, is background dependent (BD). Efforts to unify both by BI have not yielded much success. In addition, it is recognized that we cannot consider gravity in a quantum theory by BD. This paper focuses on neither the BI method based on the invariant speed of light and the inertial mass observed only in the uniform field nor the method to consider gravity in an existing quantum theory. By using the invariant mass and the speed of light in the frame of reference of the free space of the electromagnetism as well as the observed variable mass and wave speed, a method to link them to the equivalence of light's momentum was explained. In addition, some cases in which we can observe space from a micro-world by the equivalence principle were examined.

Key words: Background independent, gravity, free space, electromagnetism, invariant mass, variable mass, speed of light, wave speed.

INTRODUCTION

In this paper, given the established principles of electromagnetism, they were logically and rationally integrated with those of mechanics. The electromagnetic correlation between the speed and energy of light was defined and interrelated with the mechanics of the energy, momentum, mass, and speed of light. The question of whether gravity should be taken into consideration in the electromagnetic analysis of free space and vacuums is also addressed. Moreover, a deviation was made from the approach of the theory of relativity, which unifies electromagnetism and mechanics by disregarding gravity and assuming that the speed of light is constant. The two fields were unified by considering the interrelation of gravity and mass and assuming a fixed speed of light in free space. This assumption is the most important aspect of the proposition of this paper.

Firstly, the known facts of classical physics were stated, including (1) the speed and energy of light waves, and (2) the mass and velocity of a material in free space. Some unique terms and symbols used in this paper were also defined, highlighting the difference between particle velocity (v) and wave speed (w) and went further to discuss the following issues about gravity, based on the assumptions already made:

i. Gravitational mass and the light wave speed under gravity.

E-mail: s_hyama@yahoo.co.jp, Tel: +81-70-6611-3358, Fax: +81-70-6611-3358.

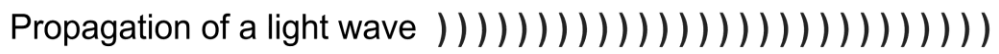

Figure 1. Propagation of a light wave.

ii. Mass and velocity of a material under gravity.
iii. Mass and speed of photons under gravity.
iv. The speed of light and the wave speed are different physical quantities.
v. Matter wave and uncertainty relation.

Finally, a conclusion from the abovementioned considerations was derived, and the correlation of speed, mass, momentum, energy, and quantum in the context of logical and rational integration of electromagnetism and mechanics were summarized. This integration is based on the interrelation of the physical quantities in terms of the equivalence principle by the momentum of light.

SPEED AND ENERGY OF LIGHT WAVES WITHOUT TAKING GRAVITY INTO CONSIDERATION

In electromagnetism, free space is a virtual space where no matter exists. It is defined by physical constants such as the speed of light in a vacuum (free space), magnetic permeability of a vacuum (free space), and permittivity of a vacuum (free space). Maxwell's equation of the speed of propagation of an electromagnetic field is as follows:

$$C = 1/\sqrt{\varepsilon_0 \mu_0} \quad (1)$$

where C is the speed of light, and μ_0 and ε_0 are the permeability and permittivity of a vacuum (free space), respectively (Figure 1). The correlation between the electromagnetic wave energy (E), absolute value of the momentum of light (P), and speed of light (C) can be derived from the theory of electromagnetism alone:

$$E = PC \quad (2)$$

Furthermore, in the MKSA system or the International System of Units (SI), the absolute refractive index n_0 is obtained by dividing the speed of light in a vacuum (free space) (C) by the light wave speed in a medium (w). In other words, it is given by the phase speed.

$$n_0 = \frac{C}{w} = \sqrt{\frac{\varepsilon\mu}{\varepsilon_0 \mu_0}} \quad (3)$$

where μ, ε are the permeability and permittivity of the medium, respectively. It can be observed from the above that the light wave speed in a medium changes and is refracted relative to the speed of light in a vacuum (free space).

VELOCITY AND INERTIAL MASS OF MATTER WITHOUT TAKING GRAVITY INTO CONSIDERATION

According to the observations of Kaufmann's experiments on bending beta rays (Boorse and Motz, 1966), the inertial mass (m') varies when the velocity (v) of the center of gravity of an object's rest mass (m_0) changes (Figure 2).

$$\frac{m'}{m_0} = \frac{C}{\sqrt{C^2 - v^2}} = \frac{1}{\sqrt{1 - v^2/C^2}} \quad (4)$$

The momentum of light (P) is obtained from the correlation among the speed of light in free space (C), particle velocity (v), and wave speed (w):

$$P = m_0 C = m'\sqrt{C^2 - v^2} = m'w \quad (5)$$

The energy (E) is obtained by multiplying the momentum of light by the speed of light (C):

$$E = PC = m_0 C^2 = m_0(v^2 + w^2) = m'wC \quad (6)$$

GRAVITATIONAL MASS AND LIGHT WAVE SPEED UNDER GRAVITY

If we consider free space as the standard, Earth's substances would exert a gravitational influence on the matter field of the surface. If the propagation speed of the light waves observed on Earth's surface is (w) and the gravitational potential on Earth's surface is given by $2\phi = 2GM/r$, then the sum (Equation 8) of the gravitational potential corresponds to the speed of light (C) in free space. It can thus be determined from the equation for the fixed speed of light (Equation 1) that the light wave speed decreases with increasing gravity (Figure 3).

$$w = f\lambda \quad (7)$$

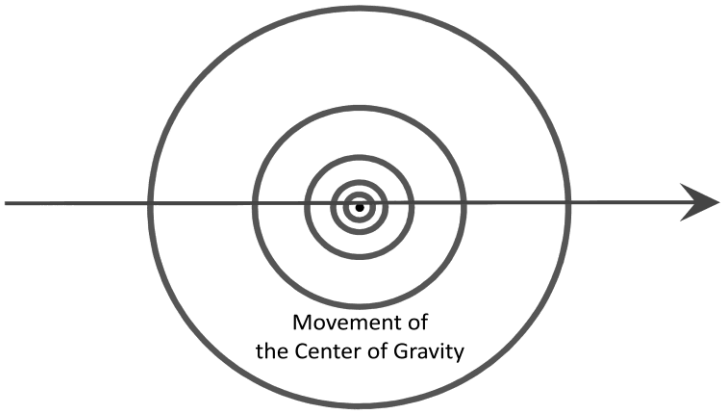

Figure 2. Movement of mass.

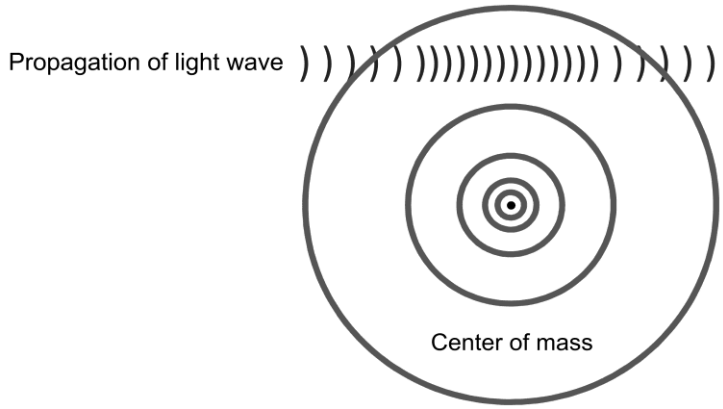

Figure 3. Perturbation between a light wave and a mass.

where f is the frequency of the wave and λ, the wavelength

.

$$C^2 = w^2 + 2\varphi \tag{8}$$

Gravitational mass (M) is the product of the material density ($C^2 - w^2$) and the radius (r) of the earth divided by the constant (2G). Therefore, there is no mass (M = 0) if there is no volume (r = 0).

$$M = (C^2 - w^2)\, r/2G = {v_2}^2\, r/2G \tag{9}$$

$$C^2 = w^2 + 2\varphi = {v_2}^2 + w^2 \tag{10}$$

This is equivalent to the potential (${v_2}^2 = 2GM/r$) of the second cosmic velocity (v_2).

MATERIAL MASS AND VELOCITY UNDER GRAVITY

If the object's gravitational mass (M) is considered to be equal to the inertial mass (m) of its particle motion (v^2,2φ), then the difference between the rest mass under gravity (m_0) and the inertial mass (m') can be obtained from the following:

$$C^2 = (v^2 + w^2) + 2\varphi \tag{11}$$

$$\frac{m'}{m_0} = \frac{\sqrt{C^2 - 2\varphi}}{\sqrt{C^2 - v^2 - 2\varphi}} = \frac{w_0}{w'} \tag{12}$$

$$n_0 = \frac{m}{M} = \frac{C}{\sqrt{C^2 - v^2 - 2\varphi}} = \frac{C}{w} \tag{13}$$

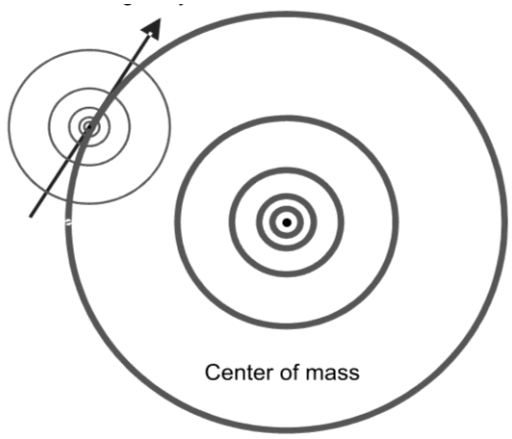

Figure 4. Perturbation in the movement of a mass.

Like the refraction rate n_0 of (Equation 3), n_0 of (Equation 13) also corresponds to the fixed speed of light in (Equation 1) (Figure 4). Furthermore, regarding the correlation between the momentum of light (P) and the energy (E), there is no equivalence between the gravitational mass and the inertial mass (M = m); however, an equivalent based on the momentum of light ($P = MC = mw$) can be obtained:

$$P = MC = m\sqrt{C^2 - v^2 - 2\varphi} = mw \quad (14)$$

$$E = PC = MC^2 = M(v^2 + w^2 + 2\varphi) = mwC \quad (15)$$

When stationary under gravity (v = 0), we can obtain an approximation of the kinetic energy ($mv^2/2$) on the basis of Newtonian mechanics:

$$E = M_2C^2 = M_2(w^2 + 2GM_1/r) \quad (16)$$

$$GM_1M_2/r = M_2(C^2 - w^2)/2 = M_2v^2/2 = m_2v^2/2n_0 \quad (17)$$

If we use the progress of an atomic clock installed in a GPS satellite as an example (Ashby, 2007),

Light wave speed on Earth's surface
$w_0 = 299,792,458\ m/s$
Geocentric gravitational constant
$GM = 3.986 \times 10^{14}\ m^3/s^2$
Radius of Earth $r = 6,378,000\ m$
Altitude of GPS satellite $h = 20,200,000\ m$
Orbital velocity of GPS satellite $v = 3,874\ m/s$
Wave speed of GPS satellite $w' = \sqrt{C^2 - v^2 - 2GM/(r+h)}$ (19)
Progress of clock $w'/w_0 = 1 + (4.45 \times 10^{-10})$ (20)

Speed of light in free space $C = \sqrt{w_0^2 + 2GM/r}$ (18)

SPEED AND MASS OF PHOTONS UNDER GRAVITY

The following can be derived from Einstein's photon hypothesis and the electromagnetic wave energy of (Equation 2):

$$E = PC = hf \quad (21)$$

where h is Planck's constant and f, the frequency. Furthermore, the following can be derived from Equations 7, 15 and 21, although the frequency of the photon hypothesis is not given by $f = C/\lambda$ but by $f = w/\lambda$.

$$hf = mwC = mCf\lambda \quad (22)$$

$$\lambda = \frac{h}{mC} \quad (23)$$

This is also understandable from the Compton Effect (Greiner, 2001a). When a material is exposed to X-rays, some of the rays are scattered and become secondary X-rays. In the Compton Effect, the wavelengths of the secondary X-rays are larger than those of the incident ones.

$$\lambda_s - \lambda_i = \frac{h}{mC}(1 - \cos\theta) = \frac{w}{f_s} - \frac{w}{f_i} \quad (24)$$

where λ_s is the wavelength of the secondary X-rays; λ_i, the wavelength of the incident X-rays; θ, the scattering angle; f_s, the frequency of the secondary X-rays; and f_i, the frequency of the incident X-rays. In this case, energy is lost under scattering, resulting in a reduced frequency ($f_s < f_i$). Moreover, because the light wave speed (w) remains unchanged, the wavelength increases ($\lambda_s > \lambda_i$) (Figure 5).

$$E = MC^2 = M(w_0^2 + 2\varphi_0) = m_0w_0C = m_0Cf\lambda_0 = hf \quad (25)$$

$$E = MC^2 = M(w'^2 + 2\varphi') = m'\dot{w}'C = m'Cf\lambda' = hf \quad (26)$$

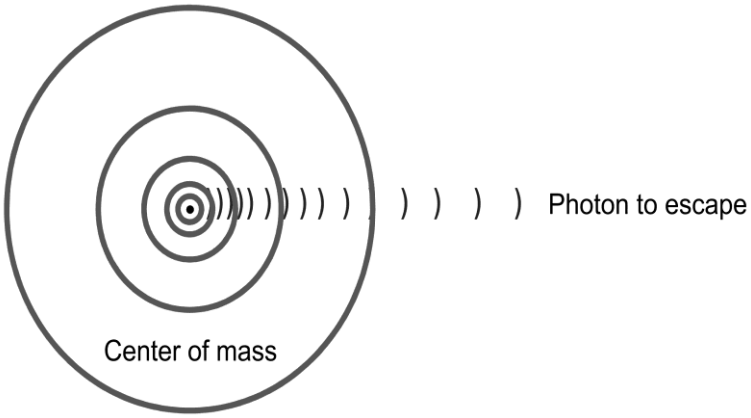

Figure 5. Photon escaping from a gravitational field.

However, with regard to the energy of the photons that escape from the gravitational field (that is, gravitational redshift), the frequency (f) remains unchanged and the gravitational potential ($\varphi_0 > \varphi'$) decreases, resulting in an increase in the light wave speed ($w_0 < w'$). Hence the wavelength increases ($\lambda_0 < \lambda'$) and the energy Equation 21 is maintained, even with a slight decrease in the inertial mass ($m_0 > m'$).

This is similar to Equation 20, where the progress of the atomic clock installed in the GPS satellite is faster than that of a clock on Earth's surface, owing to the weakened gravitational pull of the GPS satellite. This indicates that the propagated photon should be handled in the same manner as a material with mass.

SPEED OF LIGHT AND WAVE SPEED ARE DIFFERENT PHYSICAL QUANTITIES

The Shapiro Delay (Shapiro, 1964) is a combined effect of gravitational blueshift and redshift. In this phenomenon, the distance and frequency do not change, and the electromagnetic wave speed is only reduced by the expansion and contraction of the wavelength under changes in the gravitational field. This results in a delay in the arrival time (Hosokawa, 2004).

With regard to the relationships between the positions of several bodies, the Doppler Effect and gravitational blueshift and redshift are different phenomena. It has also been suspected that the speed of an electromagnetic wave does not change with frequency and energy (Abdo et al., 2009).

For gravitational blueshift,

$$E = MC^2 = M((w\downarrow)^2 + (2\varphi\uparrow)) = (m\uparrow)C(w\downarrow) = (m\uparrow)C(\lambda\downarrow)f = hf \quad (27)$$

For gravitational redshift,

$$E = MC^2 = M((w\uparrow)^2 + (2\varphi\downarrow)) = (m\downarrow)C(w\uparrow) = (m\downarrow)C(\lambda\uparrow)f = hf \quad (28)$$

For Doppler blueshift,

$$\uparrow E = (M\uparrow)C^2 = (M\uparrow)(w^2 + 2\varphi) = (m\uparrow)Cw = (m\uparrow)C(\lambda\downarrow)(f\uparrow) = h(f\uparrow) \quad (29)$$

For Doppler redshift,

$$\downarrow E = (M\downarrow)C^2 = (M\downarrow)(w^2 + 2\varphi) = (m\downarrow)Cw = (m\downarrow)C(\lambda\uparrow)(f\downarrow) = h(f\downarrow) \quad (30)$$

In the above equations, E is the energy; M, the gravitational mass; C, the speed of light; w, the electromagnetic wave speed; 2φ, the gravitational potential; h, Plank's constant; f, the frequency; m, the inertial mass; and λ, the wavelength.

The ratio of the speed of light to the wave speed is the same as the ratios of the progress of the clock. The ratios of the progress of the clock and the wave propagation speed are constant relative to stationary observer under given conditions, and the speed of light is always the same.

$C = (C/w)\, f\lambda$

However, the propagation speed of the electromagnetic wave changes with the position of the observer and with the conditions.

$C/w = n$: index of refraction

This is similar to how the propagation speed of light waves changes in different mediums.

$C/n = w = f\lambda$

In a sense, this can be used to determine when a

Table 1. Comparison according to the theory of lens and redshift.

Theory	Gravitation	Weak field→				→Strong field→				→Weak field (observer)			
	Phenomenon	Wave length	Frequency	Velocity	Energy	wl	f	v	e	wl	f	v	e
General theory of relativity	Lens	—	—	C	—	↓	↑	C	↑	—	—	C	—
	Redshift					—	—	C	—	↑	↓	C	↓
This paper	Lens	—	—	w	—	↓	—	↓	—	—	—	w	—
	Redshift					—	—	w	—	↑	—	↑	—

gravitational field is not a perfect vacuum (free space) and contains matter. If the binding energy is generated by the perturbation of objects separated by a distance, the potential energy would be restored. The equivalence principle of the momentum of light precisely relates all energy forms in space-time.

$C = d/t$

In the above equation, d is the distance and t, the time. A random change in the local energy can therefore be distinguished from a cosmology-like space-time transformation.

MATTER WAVE AND UNCERTAINTY RELATION

It is not incorrect for the relation E = hf to be complete in a matter wave (Greiner, 2001b). It is incorrect to ignore both the light wave and the matter wave as a Lorentz invariance without the equivalence principle and correlation expecting relations, namely, v = fλ or C = fλ. The speed of the quantum, which changes to a different type, is expressed as given below. The energy speed of each quantum is the speed of light.

$$C^2 = v^2 + w_1^{\,2} \rightarrow C = w_2 \quad (31)$$

In the matter wave, a wavelength (speed) change and an inertial mass change have an inverse relation in a manner similar to the gravitational red (blue) shift of the electromagnetic wave.

$$E = MC^2 = M((\Delta w)^2 + (\Delta 2\varphi)) = (\Delta m)C(\Delta w) = (\Delta m)C(\Delta \lambda)f = nhf \quad (32)$$

The reference time that we set artificially does not fluctuate. Therefore, energy and time do not show uncertainty relations. An observable result of the energy fluctuates from the space-time of the established reference. Even if the wave speed of the quantum fluctuates under gravity uncertainly, Planck's constant remains, and is the reason called the Hertzian oscillator.

The inverse relation of a wavelength (speed) change and an inertial mass change is similar to the group speed of the mixed wave and the relations of the phase velocity, and photons, matter waves, neutrino oscillations (Ahn et al., 2006), and so on can all be explained by the same mechanism. In the energy expression of the wave speed, speed lower than that of light in the mass-energy equivalence of mass have some meaning (Table 1).

CONCLUSION

The principles of electromagnetism state are that the speed of light is constant in free (virtual) space and that it is expressed by variable wave speeds in different mediums. Through this paper, it has been shown that the gravitational field could be expressed by the variable wave speed in different mediums. If the speed of light is assumed constant in the mass-energy equivalence, the invariant mass corresponds to the speed of light in free space, and the variable mass and variable wave speed in the matter field and the inertial system should be combined. The rest mass measured on the surface of Earth, which is not a free space, is not invariant. The progress of the clock by the ratio of the speed of light and the wave speed and the equivalence of the two masses must be directly linked to electromagnetism for the original unification of mechanics in only one supposition (C/w = m/M). The argument about whether a light wave is twisted or whether space-time is warped is not important. The inertia of light in the background has priority over the theory of relativity. Therefore, it is important how energy is observed from the view of free space. The equivalence principle of light's momentum harmonizes observations from quantum theory to cosmology.

Summary

The speed and velocity, mass, momentum, energy, and

quantum resulting from the interrelation of the physical quantities based on the equivalence principle by the momentum of light are defined as follows:

1. Speed and Velocity: The propagation speed of the light waves observed on Earth's surface is (w), and the gravitational potential (2Φ) on Earth's surface is given by Earth's mass plus the gravitational potential corresponding to the speed of light (C) in free space. ($C^2 = w^2 + 2\varphi$)
In the case of an object that has a center of gravity, the light wave speed (w) is decomposed into the particle velocity (v) and the wave speed (w). ($C^2 = v^2 + w^2 + 2\varphi$)

2. Mass: The invariable gravitational mass (M) is proportional to the square of the speed of light (C^2) and is the amount of matter that corresponds to the law of universal gravitation. The variable inertial mass (m) is proportional to the light wave speed (w) and is the amount of matter that corresponds to the law of conservation of momentum and Newtonian mechanics.

3. Momentum: The momentum of light (P), momentum (MC) obtained from the invariable gravitational mass (M) and the speed of light (C), and momentum (mw) obtained from the variable inertial mass (m) and the light wave speed (w) are all equivalent (that is, $P = MC = mw$) and correspond to the momentum of the material conforming to the conservation of momentum and the laws of motion of Newtonian mechanics.

4. Energy: For a substance that obeys the law of conservation of energy, the total energy (E) is calculated using the square of the speed of light (C^2) and the invariant mass (M), whereas the particle energy is calculated using the velocity (v) of the center of gravity, light wave speed (w), gravitational potential (2ϕ), speed of light (C), and momentum of light (P).
$$E = PC = MC^2 = M(v^2 + w^2 + 2\varphi) = mwC$$

5. Quantum: The digital measurement of energy (E) is satisfied with the law of conservation of energy using the product of Planck's constant (h), frequency ($f = w/\lambda$), and quantum number (n).
$$E = PC = MC^2 = mwC = nhf$$

ACKNOWLEDGEMENTS

Author would like to express his gratitude to all those who advised him on Internet forums and inquiry sites. Would also like to thank Editage for providing editorial assistance.

REFERENCES

Abdo AA, Ackermann M, Ajello M, Asano K, Atwood WB, Axelsson M, Baldini L, Ballet J, Barbiellini G, Baring MG, Bastieri D, Bechtol K, Bellazzini R, Berenji B, Bhat PN, Bissaldi E, Bloom ED, Bonamente E, Bonnell J, Borgland AW (2009). A limit on the variation of the speed of light arising from quantum gravity effects. Nature. 462(7271):331-334.

Ahn MH, Aliu E, Andringa S, Aoki S, Aoyama Y, Argyriades J, Asakura K, Ashie R, Berghaus F, Berns HG, Bhang H, Blondel A, Borghi S, Bouchez J, Boyd SC, Burguet-Castell J, Casper D, Catala J, Cavata C, Cervera A, Chen SM, Cho KO, Choi JH, Dore U, Echigo S, Espinal X, Fechner M, Fernandez E, Fujii K, Fujii Y, Fukuda S, Fukuda Y, Gomez-Cadenas J, Gran R, Hara T, Hasegawa M, Hasegawa T, Hayashi K, Hayato Y, Helmer RL, Higuchi I, Hill J, Hiraide K, Hirose E, Hosaka J, Ichikawa AK, Ieiri M, Iinuma M, Ikeda A, Inagaki T, Ishida T, Ishihara K, Ishii H, Ishii T, Ishino H, Ishitsuka M, Itow Y, Iwashita T, Jang HI, Jang JS, Jeon EJ, Jeong IS, Joo KK, Jover G, Jung CK, Kajita T, Kameda J, Kaneyuki K, Kang BH, Kato I, Kato Y, Kearns E, Kerr D, Kim CO, Khabibullin M, Khotjantsev A, Kielczewska D, Kim BJ, Kim HI, Kim JH, Kim JY, Kim SB, Kitamura M, Kitching P, Kobayashi K, Kobayashi T, Kohama M, Konaka A, Koshio Y, Kropp W, Kubota J, Kudenko Yu, Kume G, Kuno Y, Kurimoto Y, Kutter T, Learned J, Likhoded S, Lim IT, Lim SH, Loverre PF, Ludovici L, Maesaka H, Mallet J, Mariani C, Martens K, Maruyama T, Matsuno S, Matveev V, Mauger C, McConnel Mahn KB, McGrew C, Mikheyev S, Minakawa M, Minamino A, Mine S, Mineev O, Mitsuda C, Mitsuka G, Miura M, Moriguchi Y, Morita T, Moriyama S, Nakadaira T, Nakahata M, Nakamura K, Nakano I, Nakata F, Nakaya T, Nakayama S, Namba T, Nambu, R, Nawang S, Nishikawa K, Nishino H, Nishiyama S, Nitta K, Noda S, Noumi H, Nova F, Novella P, Obayashi Y, Okada A, Okumura K, Okumura M, Onchi M, Ooyabu T, Oser, SM, Otaki T, Oyama Y, Pac MY, Park H, Pierre F, Rodriguez A, Saji C, Sakai A, Sakuda M, Sakurai N, Sanchez F, Sarrat A, Sasaki T, Sato H, Sato K, Scholberg K, Schroeter R, Sekiguchi M, Seo E, Sharkey E, Shima A, Shiozawa M, Shiraishi K, Sitjes G, Smy M, So H, Sobel H, Sorel M, Stone J, Sulak L, Suga Y, Suzuki A, Suzuki Y, Suzuki Y, Tada M, Takahashi T, Takasaki M, Takatsuki M, Takenaga Y, Takenaka K, Takeuchi H, Takeuchi Y, Taki K, Takubo Y, Tamura N, Tanaka H, Tanaka K, Tanaka M, Tanaka, Y, Tashiro K, Terri R, T'Jampens S, Tornero-Lopez A, Toshito T, Totsuka Y, Ueda S, Vagins M, Whitehead L, Walter CW, Wang W, Wilkes RJ, Yamada S, Yamada Y, Yamamoto S, Yamanoi Y, Yanagisawa C, Yershov N, Yokoyama H, Yokoyama, M, Yoo J, Yoshida M, Zalipska J (2006). Measurement of neutrino oscillation by the K2K experiment. Phys. Rev. D 74:072003. hep-ex/0606032.

Ashby N (2007). Relativity in the global positioning system. Living Rev. Relativity 6.

Boorse HA, Motz L (1966). The World of the Atom. Basic Books, Inc., pp. 502-512.

Greiner W (2001a). The Quantization of Physical Quantities, Quantum Mechanics: An Introduction. Springer, pp. 1-8.

Greiner W (2001b). Wave Aspects of Matter, Quantum Mechanics: An Introduction. Springer, pp. 29-66.

Hosokawa M (2004). 2 Basics of time and frequency standard 2-3 Relativisitic effects in time and frequency standards. Review of the Communications Research Laboratory 49(1/2):15-23.

Shapiro II (1964). Fourth test of general relativity. Phys. Rev. Lett. 13(26):789-791.

academicJournals

Related Journals Published by Academic Journals

- African Journal of Mathematics and Computer Science Research
- African Journal of Pure and Applied Chemistry
- Journal of Geology and Mining Research
- Journal of Environmental Chemistry and Ecotoxicology
- Journal of Internet and Information Systems
- Journal of Oceanography and Marine Science
- Journal of Petroleum Technology and Alternative Fuels